Chapter 5

A Unified Creep-Fatigue Equation with Application to Engineering Design

Dan Liu and Dirk John Pons

Additional information is available at the end of the chapter

http://dx.doi.org/10.5772/intechopen.70877

Abstract

Background: Creep-fatigue damage occurs under cyclic loading at elevated temperature. The existing creep-fatigue models have limited ability to cover the full combination of creep and fatigue behaviours, except with extensive prior empirical testing. Consequently, they cannot effectively and efficiently be used for early engineering design.

Approach: We present a strain-based unified creep-fatigue formulation that overcomes these limitations. We validate this equation against empirical data for multiple materials, and shows it is able to cover full ranges from pure fatigue to pure creep. A simplified formulation is developed where the coefficients are extracted through simple creep-rupture tests. We show how the equation may be used in a design situation, by application to a representative gas turbine blisk. Included here is a demonstration of how the equation may be integrated into finite element analysis, which is an important practical consideration in the design work flow.

Outcomes: The results demonstrate that the unified equation evidences fidelity to empirical data for creep-fatigue behaviours for multiple metallic materials. The usefulness of this equation is the ability to identify candidate materials for creep-fatigue loading situations. The ability to achieve this at relatively early design stages is advantageous because of the economy and convenience provided.

Keywords: creep-fatigue, accuracy, economy, engineering design, turbine blisk

1. Introduction

Creep-fatigue failure results from the interaction of pure fatigue and creep, and is influenced by temperature, frequency and applied loading. The conventional strain-based creep-fatigue equations are quantitatively accurate in narrow areas of application, but suffer from poor ability to generalize to other materials and loading regimes. Consequently, those equations are ineffective and inefficient for engineering design. A recent development in the field is a

unified formulation of creep-fatigue. The advantages of this unified creep-fatigue equation are that it accommodates the crucial parameters (temperature, frequency and loading), covers different materials, represents the full range of conditions from pure fatigue to pure creep and is economical in the testing regime to determine coefficients. This chapter describes the unified creep-fatigue equation and applies it to design. The theory can be applied to evaluate the fatigue capacity of candidate materials at the early stages of design.

2. Desirable characteristics of a creep-fatigue method for design

For the perspective of engineering design, the development of a creep-fatigue method should consider following four areas:

2.1. Unified characteristic

The unified characteristic is defined as the ability to predict fatigue life for multiple temperatures and cyclic times for multiple materials. In this case, the desirable formulation should accommodate all relevant variables (including temperature, cyclic time and applied loading), and should present small difference between predicted life and experimental result under multiple situations.

2.2. Integrated characteristic

The integrated characteristic refers to the ability to cover full range of conditions from pure-fatigue condition to pure-creep condition. In this case, the desirable formulation should have the ability to be transformed to the representations of pure fatigue and pure creep, and the transformed formulations should be consistent with the general understanding of fatigue and creep mechanisms.

2.3. Economy

A desirable engineering method for fatigue-life prediction should present good balance between accuracy and economy. The economy of this theory can be assessed by evaluating the life-prediction error with overall experimental cost. Generally, the higher sensitive a numerical formulation has, the more experimental data are needed and the poorer economy is presented.

2.4. Applicability to engineering design

An engineering-based creep-fatigue method should be effectively and efficiently applicable to practical design process, where an economical, convenient and accurate method is represented to engineers and designers. Such as, the creep-fatigue evaluation by using this formulation is applied to the initial stage of design to select material or optimize structure.

Overall, a desirable creep-fatigue formulation for engineering design should have unified and integrated characteristics, and present good economy and applicability to practical design.

http://dx.doi.org/10.5772/intechopen.70877

3. Brief review of existing creep-fatigue models

Creep-fatigue behavior is generally influenced by temperature and frequency/cyclic time, wherein increasing temperature or decreasing frequency results in reduced fatigue capacity due to intensified creep damage. Normally, the existing creep-fatigue equations were derived from empirical data through curve fitting, and present the extension of the Coffin-Manson equation (Eq. (1)) [1, 2]:

$$\Delta\varepsilon_p/2 = \varepsilon_f'\left(2N_f\right)^{\beta} \tag{1}$$

where $\Delta\varepsilon_p$ is the plastic amplitude, ε_f' is the fatigue ductility coefficient, β is the fatigue ductility exponent and N_f is the cycles to failure. The development of creep-fatigue model was firstly attempted by Coffin, who proposed the frequency-modified Coffin-Manson equation (Eq. (2)) [3]:

$$\varepsilon_p = C\left(N_f f^{k-1}\right)^{-\beta_0} \tag{2}$$

where f is the frequency and k is a constant obtained from experiments and is given different values for different temperatures (temperature dependency is indirectly introduced). Then, through directly integrating with temperature dependence, the frequency-modified Coffin-Manson equation (Eq. (2)) was further developed to show the combined influence of temperature on creep-fatigue. For example, Solomon proposed a creep-fatigue equation (Eq. (3)) [4] for Sn40Pb solder:

$$\varepsilon_p = C_1(T)\left(N_f f^{k-1}\right)^{-\beta_0} \tag{3}$$

with

$$C_1(T) = 1.338 - 2\times10^{-4}T - 1\times10^{-5}T^2 - 2\times10^{-7}T^3$$

where T is the temperature, $\beta_o = 0.5$ and k is the constant and related to the frequency: $k = -0.42$ for 6×10^{-5} Hz $\leq f \leq 3\times10^{-4}$ Hz and $k = -0.84$ for 3×10^{-4} Hz $\leq f \leq 0.3$ Hz. In addition, based on the creep-fatigue tests on 63Sn37Pb solder, Shi et al. presented a creep-fatigue formulation (Eq. (4)) [5]:

$$\varepsilon_p = C_2(T)\left[N_f f^{k(T)-1}\right]^{-\beta_0(T)} \tag{4}$$

with

$$C_2(T) = 2.122 - 3.57\times10^{-3}T + 1.329\times10^{-5}T^2 - 2.502\times10^{-7}T^3$$

$$\beta_0(T) = 0.731 - 1.63\times10^{-4}T + 1.392\times10^{-6}T^2 - 1.151\times10^{-8}T^3$$

$$k_1(T) = 0.919 - 1.765\times10^{-4}T - 8.634\times10^{-7}T^2$$

$$k_2(T) = 0.437 - 3.753\times10^{-4}T - 8.04\times10^{-7}T^2$$

where $k_1(T)$ and $k_2(T)$ are the frequency-exponent functions for 10^{-3} Hz < f < 1 Hz and 10^{-4} Hz < f < 10^{-3} Hz, respectively.

Not all strain-based creep-fatigue models follow the pattern of the frequency-modified Coffin-Manson equation. For example, Jing et al. proposed a temperature-modified Coffin-Manson equation (Eq. (5)) [6], wherein the temperature dependence is incorporated into the coefficient and exponent of the Coffin-Manson equation, respectively.

$$\Delta\varepsilon_p/2 = C_3\left(2N_f\right)^{\beta} \tag{5}$$

with

$$C_3(T) = 68.79 - 0.34T + 250.56/\sqrt{T}$$

$$\beta(T) = 1.29 - 0.0053T + 2.5/\sqrt{T}$$

In addition, the creep-fatigue model (Eq. (6)) [7] developed by Engelmaier presents the influence of both temperature and frequency on creep-fatigue, where a logarithmic relationship between temperature and frequency is included.

$$\varepsilon_p = C_4 {N_f}^{-\beta_0\left(\overline{T},f\right)} \tag{6}$$

with

$$\beta_0\left(\overline{T},f\right) = 0.442 + 6\times10^{-4}\overline{T} - 1.74\times10^{-2}\ln\left(1+43200f\right)$$

where $\overline{T}$ is the mean temperature and f is the cyclic frequency ($1 \le f \le 1000$ cycles/day).

Besides temperature and frequency, applied loading also contributes to creep damage. This factor was considered by Wong and Mai, and then they proposed a unified creep-fatigue equation (Eq. (7)) [8] which accommodates temperature, frequency and applied loading.

$$\varepsilon_p = C_0 s(\sigma) c(T,f) {N_f}^{-\beta_0 b(T,f)} \tag{7}$$

with

$$s(\sigma) = \begin{cases} 1 & \textit{when creep is dormant} \\ \exp\left[-\left(\sigma_{yield}\varepsilon_p^{n'}\right)/A\right] & \textit{when creep is active} \end{cases}$$

$$c(T,f) = 1 - c_1\left(T - T_{ref}\right) - c_2\log\left(f/f_{ref}\right)$$

$$b(T,f) = 1 - b_1\left(T - T_{ref}\right) - b_2\log\left(f/f_{ref}\right)$$

where n' is the cyclic hardening index, A, c_1, c_2, b_1 and b_2 are the positive constants, T_{ref} is the reference temperature below which creep becomes dormant and f_{ref} is the reference frequency above which creep becomes dormant.

Overall, the existing creep-fatigue formulations were developed through limited empirical data for specific materials, and not all models accommodate both temperature and frequency dependencies. Consequently these derivations and models may not be extended to predict fatigue life for multiple temperatures, frequencies or different materials, thus cannot present a unified characteristic. Theoretically, the existing models may show the unified characteristic by recalculating the coefficients for each new material encountered. However, this would merely provide a numerical model without a fundamental physical theory. Furthermore such an approach would be poor economy due to the empirical effort involved.

In addition, these existing models only describe creep-fatigue behavior, and cannot cover the full range of conditions from pure fatigue to pure creep. Taking Solomon's equation as an example, the pure-fatigue condition is presented by letting $C_1(T)f^{\beta(1-k)} = C_0$. When the extreme frequency is imposed, $f \to \infty$, the functions $C_1(T)$ becomes infinitely small, which causes $T \to \infty$. This does not agree with the general understanding of pure fatigue, where the temperature should be lower than 35% of the melting temperature [9]. The pure-creep condition is presented by putting $\varepsilon_p = 0$. This is satisfied by letting $C_1 = 0$, which returns $T = 172°C$. This implies creep-rupture only occur when the temperature closes to melting temperature (186°C for 60Sn40Pb), which does not agree with general understanding that creep is active at much lower temperature [9].

Furthermore, the existing creep-fatigue equations were derived from the method of curve fitting, where more coefficients were introduced to achieve high quality of fitting to empirical data. When these models are applied to describe creep-fatigue behavior for another material, a large amount of empirical effort is involved to get high fitting accuracy. In this case the outcomes are strongly sensitive to the quality and quantity of empirical data.

Finally, per Section 2, these disadvantages are significant in the case of engineering design, where decisions (such as material selection) must be made on incomplete information. Consequently, the existing methods are often not applicable to practical design process except in narrowly defined areas.

These limitations have been recently improved by the *strain-based unified creep-fatigue* equation [10, 11]. The next sections describe the advantages of this new model, and present a case study illustrating its applicability to engineering design.

4. Description of the strain-based unified creep-fatigue equation

The strain-based unified creep-fatigue equation (Eq. (8)) [10, 11] is based on the underlying physical mechanisms of fatigue and creep. It provides a linear relationship between temperature and applied loading, based on the observation of creep-diffusion phenomenon [12], and it includes a power-law relation between number of cycles and applied loading which is consistent with crack-growth behavior [13]. Structurally, this formulation presents an extension of the Coffin-Manson equation, and the creep effect is numerically incorporated based on the concept of *fatigue capacity*. This equation includes the variables of temperature, cyclic time and applied loading, and proposes that the full fatigue capacity is gradually consumed by the elevated temperature and prolonged cyclic time. The strain form is:

$$\varepsilon_p = C_0 c(\sigma, T, t_c) N^{-\beta_0} \tag{8}$$

with

$$c(\sigma, T, t_c) = 1 - c_1(\sigma)\left(T - T_{ref}\right) - c_2 \log\left(t_c / t_{ref}\right)$$

$$T - T_{ref} = \begin{cases} T - T_{ref} & for \quad T \geq T_{ref} \\ 0 & for \quad T \leq T_{ref} \end{cases}$$

$$t_c / t_{ref} = \begin{cases} t_c / t_{ref} & for \quad t_c \geq t_{ref} \\ 1 & for \quad t_c \leq t_{ref} \end{cases}$$

where ε_p is the plastic strain, N is the creep-fatigue life, T is the temperature, t_c is the cyclic time, T_{ref} is the reference temperature and is defined as 35% of melting temperature where the creep is active [9], t_{ref} is the reference cyclic time and is suggested as a small value, C_0 and β_0 are the constants which reflect the full fatigue capacity and $c_1(\sigma)$ and c_2 are the creep-related function and constant, respectively.

Function $c_1(\sigma)$ and constant c_2 are derived from creep-rupture tests which give the relationship of the Manson-Haferd parameter [14] against applied loading (σ), and the convergence point ($\log t_a$, T_a) of all $\log t$-T lines at different stresses. Then, the pure-creep condition ($\varepsilon_p = 0$) gives the formula of constant c_2 (Eq. (9)) through letting $T = T_{ref}$, and suggests function $c_1(\sigma)$ (Eq. (10)) through letting $t_c = t_{ref}$.

$$c_2 = \frac{1}{\log\left(t_a / t_{ref}\right)} \tag{9}$$

$$c_1(\sigma) = -\frac{c_2}{P_{MH}(\sigma)} \tag{10}$$

For the same amplitude of applied loading, the creep damage caused by constant stress is significantly larger than the damage resulting from reversed loading [15], thus a moderating factor f_m is introduced to compress the constant stress, then this presents an equivalent creep damage for the cyclic situation. This moderating factor is determined by the shape of loading wave, and is defined as the ratio of the average level to the peak value of applied cyclic loading. In this case, f_m is normally given as 0.6366 for the sinusoidal wave and 0.5 for a triangular wave. Then, with the strain-stress relation, function $c_1(\sigma)$ is converted into the form in terms of plastic strain (Eq. (11)):

$$c_1(\sigma) = -\frac{c_2}{P_{MH}(\sigma)} \rightarrow -\frac{c_2}{P_{MH}(\varepsilon_P)} = -\frac{c_2}{P_{MH}\left[f_{\mathrm{m}} \cdot K(T, t_c) \cdot {\varepsilon_P}^{n(T, t_c)}\right]} \tag{11}$$

where $K(T, t_c)$ and $n(T, t_c)$ are the strength coefficient and strain hardening exponent for cyclic-loading situation, respectively, and they are functions of temperature and cyclic time.

Finally, creep-fatigue data are applied to obtain the magnitudes of C_0 and β_0 through minimizing the error (Eq. (12)) between the predicted creep-fatigue life ($N_{pre,\,ij}$) and experimental results ($N_{\exp,\,ij}$):

$$error = \sum_{i,\,j} \left(\log N_{pre,\,ij} - \log N_{\exp,\,ij} \right)^2 \tag{12}$$

5. Evaluation of creep-fatigue models for design

Next we show that the strain-based unified creep-fatigue equation is applicable to multiple situations, covers the full range of fatigue-to-creep, and provides an economical method for engineering design. Comparing with the existing models, this new model shows significant advantages on these three areas.

5.1. The unified characteristic

Generally, the existing creep-fatigue models shown in Section 3 present good ability of fatigue-life prediction in the field where they were derived. However, the accuracy reduces when these models are extended to other materials at multiple temperatures and cyclic times. This limitation is improved by the strain-based creep-fatigue equation, which presents a general formulation based on physical mechanisms of fatigue and creep. Theoretically, the existing creep-fatigue models may also present unified characteristic through recalculating the coefficients for different materials, but the economy becomes poor which is not desired for engineering design.

The unified characteristic for the strain-based unified creep-fatigue equation is validated on multiple materials (including low melting temperature material: 63Sn37Pb solder, and high melting temperature materials: stainless steel 304, Inconel 718 and GP91 casting steel) at multiple temperatures and cyclic times. The coefficients of the unified formulation for these materials are obtained by the method shown in Section 4, and the results are presented below.

5.1.1. 63Sn37Pb solder

The coefficients of the unified formulation for 63Sn37Pb solder is shown in **Table 1** based on the creep-rupture data [16] and creep-fatigue data [5]. This material was validated in our previous research [11], but the coefficients are recalculated here since the derivation method was further improved in the present work.

C_0	β_0	c_2	T_{ref} (K)	t_{ref} (s)	f_m	Convergent point	Average error
7.894	0.825	0.1215	160	1	0.6366	(160 K, 8.232)	0.003301
$c_1(\sigma)$	$9.9586 \times 10^{-4} + 1.01122 \times 10^{-4} \cdot f_m \cdot \sigma + 8.09657 \times 10^{-7} \cdot {f_m}^2 \cdot \sigma^2$						

Table 1. Coefficients of the unified formulation for 63Sn37Pb solder.

5.1.2. Stainless steel 304

The coefficients of the unified formulation for stainless steel 304 is shown in **Table 2** based on the creep-rupture data [17] and creep-fatigue data [18].

5.1.3. Inconel 718

The coefficients of the unified formulation for Inconel 718 is shown in **Table 3** based on the creep-rupture data [19] and creep-fatigue data [20].

5.1.4. GP91 casting steel

The coefficients of the unified formulation for GP91 casting steel is shown in **Table 4** based on the creep-rupture data [21] and creep-fatigue data [22].

The validation on the above four materials shows that the strain-based unified creep-fatigue equation has the ability to cover multiple materials and presents good fatigue-life prediction at multiple temperatures and cyclic times. Structurally, Wong and Mai's equation also provides a general form, thus may have chance to present unified characteristic. In particular, the coefficients are not fixed across multiple materials, hence have to be determined in each case. The investigation indicates that Wong and Mai's equation presents smaller average errors on the materials of 63Sn37Pb solder (0.000284), stainless steel (0.002810) and Inconel 718 (0.001585) than the unified formulation. Normally, the equation with more coefficients has better fitting for empirical data. This is the main reason for smaller average error shown by using Wong and Mai's equation.

C_0	β_0	c_2	T_{ref} (K)	t_{ref} (s)	f_m	Convergent point	Average error
0.8524	0.578	0.0666	600	1	0.5	(600 K, 15.01)	0.004257
$c_1(\sigma)$	$8.5843 \times 10^{-4} + 9.74017 \times 10^{-6} \cdot f_m \cdot \sigma - 1.86542 \times 10^{-8} \cdot {f_m}^2 \cdot \sigma^2$						

Table 2. Coefficients of the unified formulation for stainless steel 304.

C_0	β_0	c_2	T_{ref} (K)	t_{ref} (s)	f_m	Convergent point	Average error
0.5658	0.608	0.0782	560	1	0.6366	(560 K, 12.78)	0.008643
$c_1(\sigma)$	$2.7679 \times 10^{-3} - 4.12347 \times 10^{-6} \cdot f_m \cdot \sigma + 3.91221 \times 10^{-9} \cdot {f_m}^2 \cdot \sigma^2$						

Table 3. Coefficients of the unified formulation for Inconel 718.

C_0	β_0	c_2	T_{ref} (K)	t_{ref} (s)	f_m	Convergent point	Average error
0.6879	0.667	0.0547	610	1	0.6366	(610 K, 18.28)	0.00876
$c_1(\sigma)$	$9.51808 \times 10^{-4} + 1.20344 \times 10^{-5} \cdot f_m \cdot \sigma - 1.75045 \times 10^{-8} \cdot {f_m}^2 \cdot \sigma^2$						

Table 4. Coefficients of the unified formulation for GP91 casting steel.

Theoretically, the equations of Coffin's, Solomon's, Shi's, Engelmaier's and Jing's may also have opportunity to present the unified characteristic through transforming them into general formulations. For example, Solomon's equation is rewritten as:

$$\varepsilon_p = C_1(T)\left(N_f f^{k-1}\right)^{-\beta_0} \tag{13}$$

with

$$C_1(T) = \mathrm{a} + \mathrm{b}T + \mathrm{c}T^2 + \mathrm{d}T^3$$

where a, b, c, d, k and β_0 are the constants obtained from experiments. Then, this modified formulation gives small errors (such as 0.000529 for 63Sn37Pb and 0.00103 for stainless steel 316), and even present better fatigue-life prediction than the unified formulation at some situations.

However, we cannot conclude that Wong and Mai's equation and those modified formulations are better than the strain-based unified creep-fatigue equation. To be specific, it is significant that Wong and Mai's equation and those modified formulations are introduced as many as coefficients to get good quality of fitting (such as seven independent coefficients for Wong and Mai's equation), thus the representation of creep-fatigue behavior is a numerical-based method and the accuracy highly relies on the number of empirical data. This means that more empirical data gives more accurate prediction, and thus poor economy is presented. However, only two independent coefficients in the unified formulation are derived by curve fitting. This implies less experimental effort is needed, and then a more economical method for fatigue-life prediction is given. This will be discussed in Section 5.3.

Overall, comparing with other existing creep-fatigue models, the strain-based unified creep-fatigue equation provides a better method for fatigue-life prediction at multiple situations, wherein the small average errors are given and the unified characteristic is proved.

5.2. The integrated characteristic

The integrated characteristic refers to the ability to cover full range of conditions from pure-fatigue condition to pure-creep condition. According to the concept of fatigue capacity, the full fatigue capacity (the pure-fatigue condition) is continuously consumed by the increasing creep effect to the condition of creep-fatigue, and finally to the pure-creep condition as the fatigue capacity is completely consumed. The comparison between different creep-fatigue models on the integrated characteristic is collected in **Table 5** [23].

Normally, the creep effect presents the dependence on temperature, cyclic time and applied loading, thus the creep-fatigue model should accommodate these relevant variables to show a good description of creep-fatigue. However, creep effect in the existing creep-fatigue models shown in Section 2 cannot be totally presented, specifically, only the temperature and cyclic time are included into the equations proposed by Solomon, Shi et al., and Engelmaier, only the cyclic time is presented in Coffin's equation and only the temperature is shown in Jing's equation.

Creep-fatigue models	Pure fatigue	Creep-fatigue	Pure creep
Coffin's equation (Eq. (2))	X	√	X
Solomon's equation (Eq. (3))	X	√	X
Shi's equation (Eq. (4))	X	√	X
Jing's equation (Eq. (5))	X	√	X
Engelmaier's equation (Eq. (6))	√	√	X
Wong & Mai's equation (Eq. (7))	√√	√√	X
Unified creep-fatigue equation (Eq. (8))	√√	√√	√√

√√: This equation can well describe the phenomena of this condition.
√: This equation can partly describe the phenomena of this condition.
X: This equation cannot describe the phenomena of this condition.

Table 5. The capacity of integrated characteristic.

While, Wong and Mai's equation and the unified formulation accommodate these three variables, thus they are believed to have a better fatigue-life prediction at the creep-fatigue condition (accuracy has been shown in Section 5.1). Further investigation of stress-related functions in these two equations shows that function $c_1(\sigma)$ in the unified formulation is directly derived from creep-rupture behavior, but is not for Wong and Mai's equation. Therefore, the strain-based unified creep-fatigue equation theoretically has better presentation of creep effect.

In addition, a good creep-fatigue equation also should be capable of covering two ends of creep-fatigue condition: pure-fatigue condition and pure-creep condition. However, the equations proposed by Coffin, Solomon, Shi et al., Jing, Engelmaier, and Wong and Mai do not totally satisfy this condition. On the one hand, the condition of pure fatigue is presented by letting $C_1(T)f^{\beta(1-k)} = C_0$($C_0$ is the ductility coefficient at pure-fatigue condition) for Solomon's equation, $C_2(T)f^{\beta[1-k(T)]} = C_0$ for Shi's equation and $\beta_0\left(\overline{T},f\right) = \beta_0$ (β_0 is the ductility exponent at pure fatigue condition) for Engelmaier's equation. When the extreme frequency is imposed, $f \to \infty$, the functions $C_i(T)$ and $\beta_0\left(\overline{T},f\right)$become infinitely small, which causes $T \to \infty$. In addition, the temperature component is not shown in Coffin's equation, thus the activation of creep effect in terms of temperature is ignored in this equation. These do not agree with the general understanding of pure fatigue, where the temperature should lower than 35% of melting temperature [9]. For Jing's equation, the derivation of function $C_3(T)$ is based on the material of 80Au/20Sn solder, thus a low temperature (where the creep effect is dormant) may return a reasonable value to describe full fatigue capacity. While, when this equation is applied on steel, function $C_3(T)$ yields to an impossible negative value since the temperature at the pure-fatigue condition is much higher than the situation for solder. However, the pure-fatigue condition can be well-presented by both Wong & Mai's equation and the strain-based unified creep-fatigue equation through letting $T = T_{ref}$ *and* $t = t_{ref}$, where they can be restored to the Coffin-Manson equation.

On the other hand, the condition of pure creep is presented by letting $\varepsilon_p = 0$. This condition cannot be satisfied by the equation of Coffin, because the coefficient C and exponent β_0 are constant, which leads to impossible zero time or zero frequency. In addition, for the equation of

Engelmaier, the pure-creep condition is satisfied by letting $\beta_0(\overline{T},f)\rightarrow+\infty$, which implies $T\rightarrow+\infty$. The pure-creep condition for the equations proposed by Solomon, Shi et al. and Jing et al. is satisfied by letting $C_1 = C_2 = C_3 = 0$, which returns T = 172, 198 and 249°C, respectively. The Solomon's and Jing's equations imply that creep-rupture only occur when the temperature closes to melting temperature (186°C for 60Sn40Pb solder and 280°C for 80Au/20Sn solder), while Shi's equation suggests that creep-rupture only occur above melting temperature (183°C). The creep activation temperatures obtained from these four creep-fatigue equations do not agree with general understanding of creep, where creep is active at 35% of melting temperature. Although Wong and Mai's equation has a good description for pure fatigue, it cannot present pure-creep condition entirely. This is because letting $s(\sigma)c(T_R,f_R)=0$ cannot deduce any well-known time-temperature parameters, such as the Larson-Miller parameter [24], the Sherby-Dorn parameter [25] and the Manson-Haferd parameter [14]. However, the Manson-Haferd parameter can be well-presented through letting $c(\sigma,T,t_c)=0$ for the strain-based unified creep-fatigue equation.

Overall, comparing with other existing creep-fatigue models, the strain-based unified creep-fatigue equation can cover the full range of conditions from pure fatigue to pure creep. Specifically, this equation has capability to model pure fatigue at $c(\varepsilon_p,T,t_c) = 1$ where this equation is restored to the Coffin-Manson equation, model pure creep-rupture at $c(\varepsilon_p,T,t_c) = 0$ where this equation is transformed to the Manson-Haferd parameter, and model creep-fatigue damage at $0 \le c(\varepsilon_p,T,t_c) \le 1$ where the creep effect is influenced by temperature, cyclic time and applied loading.

5.3. The economy

Engineering design of fatigue-life evaluation always requires good performance on both accuracy and economy [26]. The accuracy has been shown in Section 5.1 and the economy will be discussed in this section, where Wong and Mai's equation is select to compare with the strain-based unified creep-fatigue equation in terms of economy. The results show that the unified formulation provides a more economical method for fatigue-life prediction because the minimum experimental effort is involved.

Normally, the accuracy to predict or fit a distribution (or a trend) by a numerical formulation partly depends on the number of coefficients, which implies that the formulation with more coefficients presents better fitting [27]. However, this factor is not isolated, and is strongly related to the number of data points. Specifically, the more coefficients are introduced, then the more data points are needed to pick up, and then the better fitting can be gotten. This does not mean that a good formulation should contain as many as coefficients because this may lead to redundancy on the empirical effort. Therefore, is very important for deriving a formulation to keep a good balance between accuracy and consumption. In this case, the strain-based unified creep-fatigue equation satisfies this requirement.

As mentioned in Section 5.1, Wong and Mai's equation has seven independent coefficients which are totally obtained through numerical method, but only two independent coefficients are included in the unified formulation. This suggests that more empirical data are needed to

give better fitting for Wong & Mai's equation, but this result in poor economy since performing a large number of creep-fatigue experiments is expensive and time-consuming. This significantly is not a good choice for engineering design due to the undesirable high cost. However, when less creep-fatigue tests are involved to control the total cost, the accuracy for fatigue-life prediction remarkably reduces. This limitation is improved by using the strain-based unified creep-fatigue equation, where a better balance between accuracy and economy is given. The comparison between Wong and Mai's equation and the unified formulation on the accuracy of prediction in terms of empirical-data number is shown in **Table 6**, where the materials of 63Sn37Pb and stainless steel 304 are investigated.

Taking 63Sn37Pb solder as an example, **Table 6** shows that Wong and Mai's equation gives better accuracy on fatigue-life prediction than the unified formulation when all eight groups of creep-fatigue data are imposed, wherein the average errors are 0.000284 for Wong and Mai's equation and 0.003301 for the unified formulation. Then, three groups of creep-fatigue data (T = 233 K, t_c = 1 s; T = 298 K, t_c = 10s; T = 298 K, t_c = 1000s) were selected to extract the coefficients, and the numerical method still yields to quite small errors for fitting. However, when Wong and Mai's equation with the coefficients obtained at this stage is extended to predict fatigue life at total eight creep-fatigue situations, a poor accuracy is given, where the average error dramatically worsens to 0.2445 from 0.000284. This undesirable result is significantly improved by the strain-based unified creep-fatigue equation, wherein the difference between the average errors of fatigue-life prediction under two situations is very small (specifically, 0.003301 for the coefficients obtained from eight groups of creep-fatigue data and 0.00355 for the coefficients obtained from three groups of data). This implies that less creep-fatigue experiments may be involved to obtain the coefficients of the unified formulation, and the accuracy of fatigue-life prediction by using Wong and Mai's equation is more sensitive on the number of empirical data. Consequently, the unified equation provides a more economical method for engineering design because of the reduced number of creep-fatigue experiments. This result is further demonstrated by the material of stainless steel 304, and the average errors under two situations are shown in **Table 6**.

Overall, it is clear that the better fatigue-life prediction provided by Wong and Mai's equation (also other modified formulations from the original equations of Coffin's, Solomon's, Shi's, Engelmaier's and Jing's) is obtained through sacrificing economy. However, the strain-based

Materials	Number of data to derive coefficients	Average errors on predict fatigue life	
		Wong & Mai's equation	Unified creep-fatigue equation
63Sn37Pb	8 groups of data	0.000284	0.003301
	3 groups of data	0.2445	0.00355
Stainless steel 304	7 groups of data	0.002810	0.004257
	3 groups of data	0.4684	0.007199

Table 6. Accuracy of prediction in terms of empirical-data number.

unified creep-fatigue equation provides a more practical method of fatigue-life evaluation for engineering design, wherein a good balance between accuracy and economy is achieved.

The research conducted by Manson indicated that the Coffin-Mansion equation can be modified to a universal slops formulation (Eq. (14)) through introducing the ductility (D) based on the observation of 47 materials [28]:

$$\Delta\varepsilon_p = 0.547D^{0.43}N_f{}^{-0.5} \tag{14}$$

Significantly, the coefficients of this equation can be directly derived from material properties, thus no fatigue test is involved. This remarkably reduces the cost spent on experiments, and thus could be introduced to simplify the unified creep-fatigue equation to eliminate creep-fatigue test. According to the empirical data on the materials of Stainless steel 316, Stainless steel 304, Inconel 718 and GP91 casting steel, the simplified formulation is presented as (Eq. (15)):

$$\Delta\varepsilon_p = 0.8965D^{0.3998}c(\sigma, T, t_c)N_f{}^{-0.629} \tag{15}$$

This simplified form provides an easy way to extract the coefficients without any creep-fatigue tests, and only creep-rupture tests are needed. Therefore, a more economical method of fatigue-life prediction is proposed. This formulation could be further modified and improved if more materials are investigated. However, the solder materials are not included in this simplified form because solder materials present quite different material properties from carbon-based materials, where they has more significant deformation at break and higher full fatigue capacity [29, 30]. Therefore, the solder materials should be separately discussed to develop a simplified formulation.

6. Design application: case study for gas turbine blisk

Evaluation shown in Section 5 indicates that the strain-based unified creep-fatigue equation presents good characteristics on unifying, integration and economy. This provides an effective and efficient creep-fatigue method for engineering design at initial stage, such as material selection, structure optimization and boundary-condition determination. Generally, during the process of design, the coefficients of this unified formulation can be extracted through minimum experimental effort. Then, the coefficients can be applied to numerically evaluate creep-fatigue under service condition. In addition, finite element analysis (FEA) is frequently applied to conduct numerical analysis of creep-fatigue in different engineering components, such as heat exchanger [31, 32], turbine blade [33–35] and electronic package [36, 37]. In this case, the coefficients obtained from the unified equation also can be imported into FEA software to reduce the complexity of analysis.

A gas turbine blisk works under high temperature, and experiences repeated starting up and shutting off. This is a typical creep-fatigue situation, where damage is caused by the combination of creep effect and fatigue effect. In this case study, the theory of highly accelerated life test is

accepted to make a selection of material. In particular, the strain-based creep-fatigue equation is used to obtain the creep-fatigue-related parameters for the evaluation of creep-fatigue damage.

6.1. Methodology for fatigue-based design

This case study is based on the theory of highly accelerated life test, which is used at the initial stage of design to improve the reliability of product, such as the selection of material, the optimization of structure, and the decision of manufacturing processes. Normally, the accelerated life test is done through intensifying the influence of stress-related factors on life. Therefore, the prediction of fatigue life and creep-rupture time in this case study cannot present the real value for the failure at the operation condition, but can provide effective guidance for engineering design, for example, differentiating between different candidate solutions.

6.1.1. Loading characteristics

Generally, the total damage is accumulated by the fatigue damage caused by repeated process of starting up and shutting off, the creep damage due to elevated temperature and the damage results from vibration. Therefore, the creep-fatigue evaluation based on each operational unit is divided into three parts: regular-loading fatigue partition (repeated process of starting up and shutting off), creep partition (elevated temperature) and irregular-loading partition (vibration) (**Figure 1**).

The partition which includes vibration is not considered because the amplitude of this irregular-loading is so small that can be ignored. Therefore, this evaluation focuses on the regular-loading partition and creep partition. The fatigue damage is caused by the repeated process of starting up and shutting off, and the maximum loading appears at the 100% rotational velocity. The waveform for the loading is triangular. The cyclic time is arbitrarily

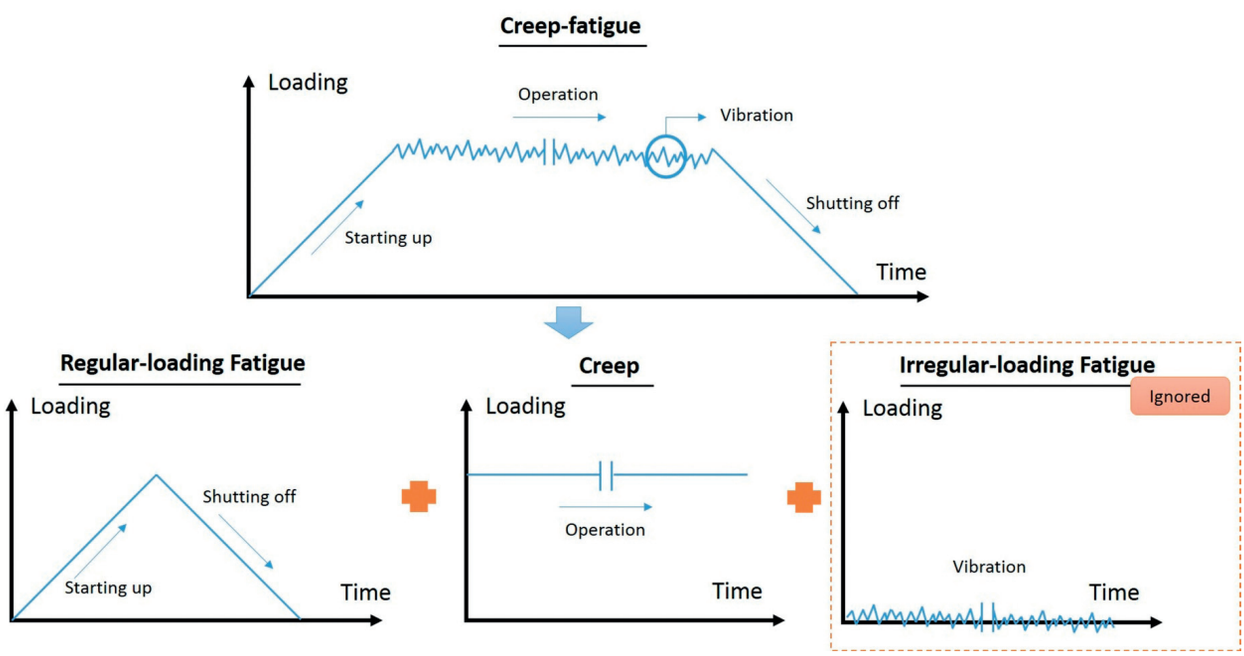

Figure 1. The partition of creep-fatigue.

defined as 1 s, which is also defined as the reference cyclic time for the strain-based creep-fatigue equation. Significantly, this small cyclic time is much smaller than the real situation, where the gas turbine blisk is impossible to start up and then shut off within 1 s. However, the choice of frequency does not influence the result of stress/strain distribution for FEA. In addition, the constant loading for creep damage at elevated temperature is defined as the applied loading at the maximum rotational velocity.

6.1.2. FEA approach

FEA methods such as ANSYS can accommodate creep, fatigue and creep-fatigue but only with data. Normally, FEA-based creep-fatigue evaluation [33, 34, 38] is based on the exploration of creep and fatigue behavior by experiments, where the relationships of creep strain versus time and applied loading versus fatigue life are imported into FEA software as engineering data to simulate creep-fatigue behavior. Then, the simulation is conducted under cyclic loading and elevated temperature. Generally, this is a complex process. This is firstly because the amount of empirical experiment required, especially the need to redo the creep test when the applied loading is changed. In addition, the introduction of a creep effect may result in non-convergence for FEA, and then the analysis settings may need to be repeatedly modified to get solution convergence. This makes it difficult to apply FEA to early design stages where the creep-fatigue material properties are not yet established empirically.

However, the complexity can be improved through using the strain-based unified creep-fatigue equation (Eq. (8)). Specifically, this new formulation is used to get the creep-fatigue-related coefficients under the service condition, then these coefficients are introduced into FEA as the engineering data. The key concept is that equation provides a method to transfer the creep effect into the creep-fatigue-related coefficients. Therefore, FEA can be conducted without the need to obtain explicit creep data. This significantly reduces the complexity of simulation. This process of substitution is described below.

The process is that the unified equation gives the creep-fatigue-related coefficients for the candidate materials under consideration. Then, the coefficients were input into ANSYS as engineering data to evaluate fatigue life. The next stage was to take the maximum stress and strain obtained from FEA and substitute into Morrow's equation. This provides another estimate of the fatigue life. Finally, the results obtained by the two methods were compared, and design implications identified. The FEA stress and strain results were also used to evaluate the creep damage using the Manson-Haferd parameter. This gives an estimate of the creep-rupture time for the creep part of the loading. The evaluation was conducted on Inconel 718 and GP91 casting steel, and the ideal material should have good performance on both fatigue and creep.

6.2. Selection of material

6.2.1. Geometry

The geometry (**Figure 2**) of gas turbine blisk was structured by Solidworks [39], and one of blades was selected to conduct FEA by using ANSYS WORKBENCH. The key dimension is shown in **Table 7**.

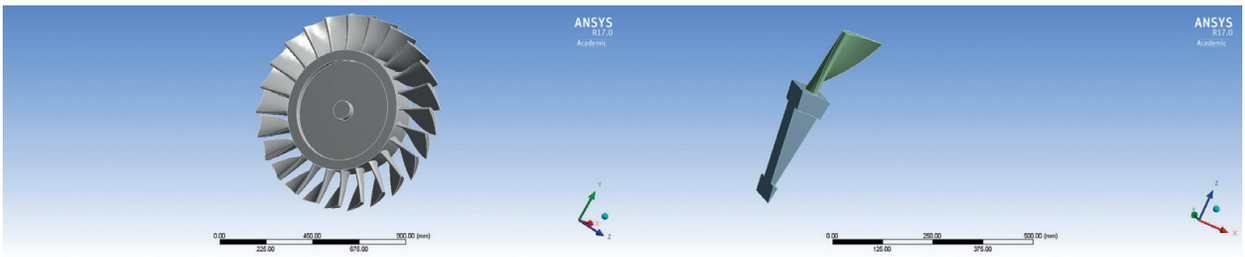

Figure 2. Geometry.

No.	Items	Dimensions
1	R_1 (the distance from center to tip of the blade)	469 mm
2	R_2 (the distance from center to root of the blade)	295 mm
3	Number of blades	24
4	The outlet anger for mean cross section	30°
5	The area of mean cross section	3036.45 mm^2

Table 7. Key dimension of geometry.

6.2.2. Service condition

The turbine blisk is working under cyclic loading and elevated temperature, and the service condition is tableted in **Table 8**:

6.2.3. Coefficients for creep-fatigue condition and material properties

According to the coefficients of the strain-based unified creep-fatigue equation for the materials of Inconel 718 shown in **Table 3** and GP 91 casting steel shown in **Table 4**, the fatigue-related coefficients at 811 K which can be input into ANSYS as engineering data are presented in **Table 9**:

In addition, the material properties of Inconel 718 [40] and GP91 casting steel [22] at 811 K are shown in **Table 10**:

6.2.4. Loading

The centrifugal force, tangential force and axial force to blades are the main loadings which cause creep-fatigue damage at elevated temperature during the repeated process of starting up and shutting off. The maximum loading is calculated at the situation of 100% rotational velocity.

Rotational velocity (n)	Temperature (T)	Mass flow rate ($\dot{M}$)	Nozzle angle (α)
3000 rpm	811 K (538°C)	31.6 kg/s	14°

Table 8. Service condition.

Materials	Strain-life relation $\Delta\varepsilon_p/2 = C(2N_f)^{\beta}$		Stress-life relation $\Delta\sigma/2 = \sigma(2N_f)^{b}$		Strain–stress relation $\Delta\sigma/2 = K(\Delta\varepsilon_p/2)^{n}$	
	C	β	σ	b	K	n
Inconel 718	0.4828	−0.636	851.6	−0.09178	946	0.1443
GP91 casting steel	0.5093	−0.662	382	−0.0422	398.5	0.0638

Table 9. The creep-fatigue-related coefficients for Inconel 718 and GP91 casting steel.

Material	Density (kg/m^3)	Yield stress (MPa)	Tensile stress (MPa)	Young's modules (MPa)
Inconel 718	8220	1069	1276	179,000
GP91 casting steel	7700	342	402	161,500

Table 10. Material properties of Inconel 718 and GP91 casting steel.

6.2.4.1. Centrifugal force

The centrifugal force can be obtained through Eq. (16) [35]:

$$F_c = 0.5\rho A\omega^2\left(R_1{}^2 - R_2{}^2\right) \tag{16}$$

where F_c is the centrifugal force, ρ is the density, A is the area of cross section and ω is the rotational velocity in rad/s. With the rotational velocity (3000 rpm), the magnitude of ω is given by Eq. (17):

$$\omega = 2\pi n/60 = 2\pi \times 3000/60 = 314.2\ rad/s \tag{17}$$

Then, the centrifugal force is presented by Eq. (18):

$$F_c = 0.5 \times 8220 \times 0.00303645 \times 314.2^2 \times \left(0.469^2 - 0.295^2\right) = 163780.776\ N \tag{18}$$

6.2.4.2. Tangential force and axial force

The tangential force and axial force are calculated through velocity triangle (**Figure 3**) [33], which is a well-accepted method for the force calculation of blade.

The mean cross section is selected to calculate the tangential force and axial force, and the results in velocity triangle are shown in **Table 11**.

Then, the tangential force (F_t) is give as (Eqs. (19) and (20)):

$$F_t = \dot{M}\Delta v_x = 31.6 \times (240.1667 + 236.17) = 15052.23972\ N \tag{19}$$

$$F_t/blade = 15052.23972/24 = 627.177\ N \tag{20}$$

and the axial force (F_a) is presented as (Eqs. (21) and (22)):

$$F_a = \dot{M}\Delta v_y = 31.6 \times (67.0645 - 59.8878) = 226.78372\ N \tag{21}$$

$$F_a/blade = 226.78372/24 = 9.449\ N \tag{22}$$

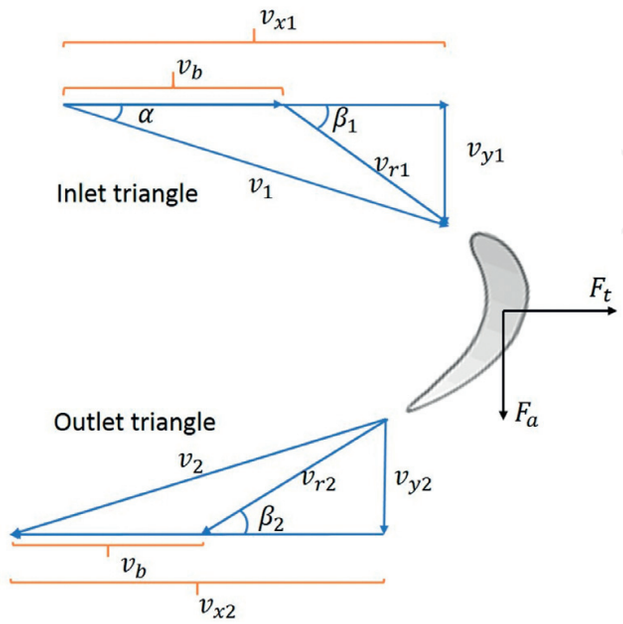

Figure 3. Velocity triangle for blade.

In the inlet triangle						**In the outlet triangle**			
v_b **(m/s)**	v_1 **(m/s)**	β_1	v_{r_1} **(m/s)**	v_{x_1} **(m/s)**	v_{y_1} **(m/s)**	v_{r_2} **(m/s)**	β_2	v_{x_2} **(m/s)**	v_{y_2} **(m/s)**
120.01	247.55	26.519^0	134.129	240.197	59.888	134.129	30^0	67.065	236.17

Table 11. The results in velocity triangle.

6.2.5. The evaluation of fatigue damage

6.2.5.1. Finite element analysis results

The finite element analysis is conducted through nonlinear analysis method [34, 35, 38]. The creep-fatigue-related coefficients from **Table 9** and the material properties from **Table 10** are input into ANSYS WORKBENCH as engineering data. The boundary condition (force) presented in Section 6.2.4 is imposed. Finally, the maximum stress, maximum total strain and fatigue life are given. The results are tabulated in **Table 12**, and fatigue-life prediction is shown in **Figure 4** for Inconel 718 and **Figure 5** for GP91 casting steel.

6.2.5.2. Predicted fatigue life through Morrow's equation

Based on the stress and strain obtained from FEA, the fatigue life can be calculated through Morrow's equation (non-zero-mean-stress condition) (Eq. (23)) [38, 41]:

http://dx.doi.org/10.5772/intechopen.70877

$$\varepsilon_t = 3.4\left(\frac{\sigma_s - \sigma_m}{E}\right){N_f}^{-0.12} + {C_0}^{0.6}{N_f}^{-0.6} \tag{23}$$

where ε_t is the total strain, σ_s is the tensile stress, E is the Young's modulus, C_0 is the fatigue ductility coefficient based on $\Delta\varepsilon_p - N$ relation and σ_m is the mean stress which is defined as the half of the maximum stress obtained from FEA.

Substituting Eq. (23) with the values obtained from FEA gives the results: N_f=2440 for Inconel 718 and N_f=348 for GP91 casting steel.

Materials	Maximum stress	Maximum total strain	Minimum fatigue life
Inconel 718	1311.8 MPa	0.011597	2350 cycles
GP91 casting steel	755.27 MPa	0.029661	327 cycles

Table 12. FEA results for Inconel 718 and GP91 casting steel.

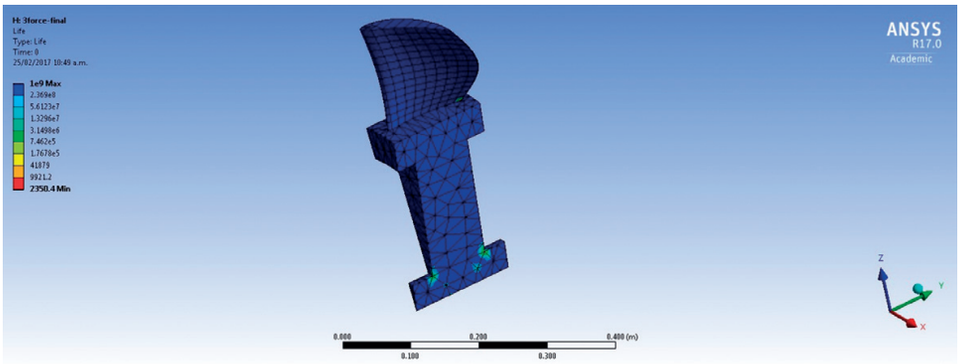

Figure 4. The fatigue life distribution for Inconel 718.

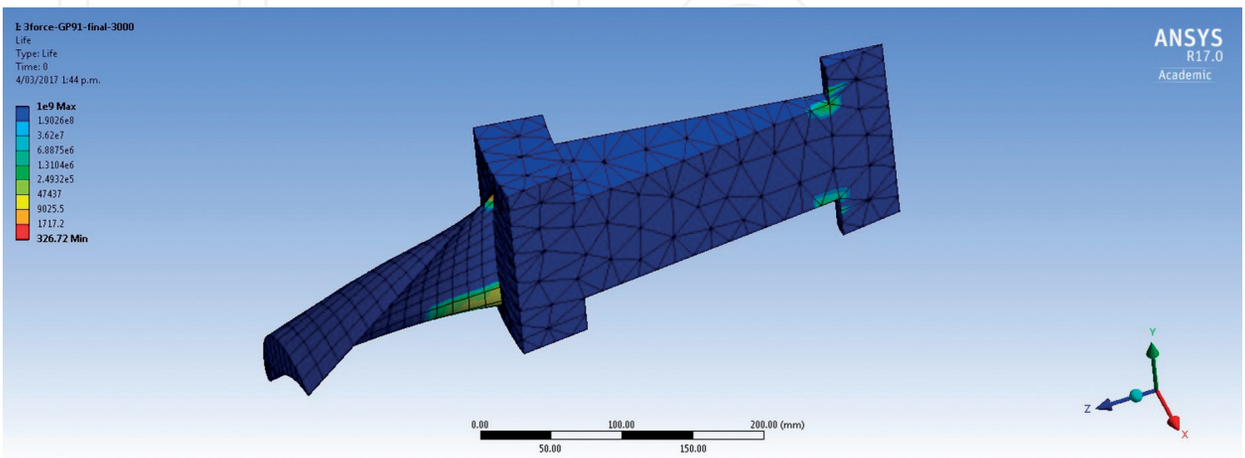

Figure 5. The fatigue life distribution for GP91 casting steel.

6.2.5.3. Comparing the results

The fatigue damage is evaluated through both FEA and the Morrow's equation, and the results are provided in **Table 13**. The error between these two results is given by Eq. (24).

$$error = \frac{N_{f-Morrow} - N_{f-FEA}}{N_{f-FEA}} \times 100\% \tag{24}$$

As shown in **Table 13**, the fatigue life obtained through Morrow's equation is higher than the result obtained from FEA. This may be because the influence of mean stress is removed from the second term (plastic strain), and thus reduces the mean-stress effect on fatigue capacity and obtains a longer fatigue-life prediction. The FEA results are more conservative, and most designers would want to proceed with them rather than the Morrow's results.

6.2.6. The evaluation of rupture time due to creep damage

According to the FEA results, the maximum plastic strain (0.005406 for Inconel 718 and 0.02498 for GP91 casting steel) can be obtained, and it could then be transformed to stress (445.4 MPa for Inconel 718 and 314.9 MPa for GP91 casting steel) by the stress-strain relation (**Table 9**). Finally, the stress is used to get the rupture time through the Manson-Haferd parameter (P_{MH}) obtained during the process of extracting the coefficients of the unified formulation. The results are shown in **Table 14**.

6.2.7. The design decision

The evaluation of fatigue damage (fatigue partition) and creep damage (creep partition) is collected in **Table 15**. The results indicate that Inconel 718 has better fatigue and creep capacity than GP91 casting steel. Therefore, Inconel 718 would be recommended as the material to take forward into the next stages of design. In safety critical situations, it would still be prudent to conduct the empirical creep-fatigue tests to validate the selection. However, it will be appreciated that conducting such tests for one material for the purposes of validation is more efficient than conducting the same tests for all candidate materials—some of which will not be taken forward.

Materials	FEA-based results	Morrow-based results	Error
Inconel 718	2350 cycles to failure	2440 cycles to failure	3.83%
GP91 casting steel	327 cycles to failure	348 cycles to failure	6.42%

Table 13. The results obtained through FEA and the Morrow's equation.

Materials	P_{MH}	$1/P_{MH}$– σ relation	Rupture time
Inconel 718	−0.0218	$-5.0 \times 10^{-8}\sigma^2 + 5.27 \times 10^{-5}\sigma - 3.5375 \times 10^{-2}$	5588 hours
GP91 casting steel	−0.0549	$3.2 \times 10^{-7}\sigma^2 - 2.2 \times 10^{-4}\sigma - 1.74 \times 10^{-2}$	4791 hours

Table 14. Creep damage for Inconel 718 and GP91 casting steel at 811 K.

Materials	Evaluation of fatigue damage	Evaluation of creep damage
Inconel 718	2350 cycles to failure	5588 hours to failure
GP91 casting steel	327 cycles to failure	4791 hours to failure

Table 15. The evaluation of fatigue damage and creep damage.

7. Limitation

The strain-based unified creep-fatigue equation was developed for the situation of zero-hold-time cyclic loading. In this case, fatigue makes more contribution than creep on failure [42], because total time is too small to produce remarkable creep damage. However, for the cyclic loading with hold time, the creep effect gradually intensifies as the hold time increases. Then, creep damage makes more contribution and the failure finally occurs due to a creep effect. Therefore, at the situation with short hold time, the unified formulation may still present a reasonable prediction of fatigue life, but the accuracy of this prediction may become worse when the hold time is prolonged.

8. Conclusion

The unified creep-fatigue equation (Eq. (8)) presents an effective and efficient method for engineering design. The advantages of this equation are:

1. Better fatigue-life prediction for multiple temperatures and cyclic times for multiple materials.
2. Ability to cover the full range of conditions from pure fatigue to pure creep.
3. Good economy since the coefficients may be determined through minimum experimental effort. Especially, a simplified form is presented where the coefficients can be obtained from simple creep-rupture tests without need for any creep-fatigue tests.
4. Applicability to engineering design and FEA.

Conflicts of interest

The authors declare no conflict of interest. The research was conducted without personal financial benefit from any funding body, and no such body influenced the execution of the work.

Author contributions

The work was conducted by DL and supervised by DP. The validation on different materials, the integrated characteristic and the economy are analyzed by DL. The case study on gas turbine blisk was conducted by DL with guidance from DP.

Author details

Dan Liu* and Dirk John Pons

*Address all correspondence to: dan.liu@pg.canterbury.ac.nz

Department of Mechanical Engineering, University of Canterbury, Christchurch, New Zealand

References

[1] Coffin LF Jr. A Study of the Effects of Cyclic Thermal Stresses on a Ductile Metal. New York, USA: Knolls Atomic Power Lab; 1953

[2] Manson SS. Behavior of Materials under Conditions of Thermal Stress. Ohio, US: Lewis Flight Propulsion Lab.; 1954

[3] Coffin L. Fatigue at High Temperature. Fatigue at Elevated Temperatures. Pennsylvania, USA: ASTM International; 1973

[4] Solomon H. Fatigue of 60/40 solder. IEEE Transactions on Manufacturing Technology. 1986;**9**:423-432

[5] Shi X, Pang H, Zhou W, Wang Z. Low cycle fatigue analysis of temperature and frequency effects in eutectic solder alloy. International Journal of Fatigue. 2000;**22**:217-228

[6] Jing H, Zhang Y, Xu L, Zhang G, Han Y, Wei J. Low cycle fatigue behavior of a eutectic 80Au/20Sn solder alloy. International Journal of Fatigue. 2015;**75**:100-107

[7] Engelmaier W. Fatigue life of leadless chip carrier solder joints during power cycling. IEEE Transactions on Components, Hybrids, and Manufacturing Technology. 1983:232-237

[8] Wong E, Mai Y-W. A unified equation for creep-fatigue. International Journal of Fatigue. 2014;**68**:186-194

[9] Ashby MF, Shercliff H, Cebon D. Materials: Engineering, Science, Processing and Design. Oxford, UK: Butterworth-Heinemann; 2013

[10] Liu D, Pons D, Wong E-H. The unified creep-fatigue equation for stainless steel 316. Metals. 2016;**6**:219

[11] Liu D, Pons D, Wong E-H. Creep-integrated fatigue equation for metals. International Journal of Fatigue. 2016;**98**:167-175

[12] Poirier J-P. Creep of Crystals: High-Temperature Deformation Processes in Metals, Ceramics and Minerals. Cambridge, UK: Cambridge University Press; 1985

[13] Weertman J. Fatigue crack propagation theories. In: Fatigue and Microstructure. Metals Park, Ohio: ASM; 1979. p. 279-206

[14] Manson S, Haferd A. A Linear Time-Temperature Relation for Extrapolation of Creep and Stress-Rupture Data. Lewis Flight Propulsion Lab; 1953

[15] Halford G. Cyclic creep-rupture behavior of three high-temperature alloys. Metallurgical Transactions. 1972;**3**:2247-2256

[16] Shi X, Wang Z, Yang Q, Pang H. Creep behavior and deformation mechanism map of Sn-Pb eutectic solder alloy. Journal of Engineering Materials and Technology. 2003;**125**:81-88

[17] Fritz LJ, Koster W. Tensile and Creep Rupture Properties of Uncoated and Coated Engineering Alloys at Elevated Temperatures. 1977

[18] Kanazawa K, Yoshida S. Effect of temperature and strain rate on the high temperature low-cycle fatigue behavior of austenitic stainless steels. Creep and Fatigue in Elevated Temperature Applications International conference sponsored by the Institution of Mechanical Engineers, American Society of Mechanical Engineers, American Society for Testing Materials, Philadelphia, 23-27 September 1973 and Sheffield, 1-5 April 1974; Vol. 11975

[19] Sugahara T, Martinolli K, Reis DA, de Moura Neto C, Couto AA, Neto FP, et al. Creep Behavior of the Inconel 718 Superalloy. Defect and Diffusion Forum. Trans Tech Publications; 2012. p. 509-514

[20] Fournier D, Pineau A. Low cycle fatigue behavior of Inconel 718 at 298 K and 823 K. Metallurgical Transactions A. 1977;**8**:1095-1105

[21] Tabuchi M, Hongo H, Li Y, Watanabe T, Takahashi Y. Evaluation of microstructures and creep damages in the HAZ of P91 steel weldment. Journal of Pressure Vessel Technology. 2009;**131**:021406

[22] Mroziński S, Golański G. Low cycle fatigue of GX12CrMoVNbN9-1 cast steel at elevated temperature. Journal of Achievements in Materials and Manufacturing Engineering. 2011;**49**:7-16

[23] Liu D, Pons D. Development of a unified creep-fatigue equation including heat treatment. Fatigue & Fracture of Engineering Materials & Structures. 2017. DOI: http://dx.doi.org/10.1111/ffe.12670

[24] Larson FR, Miller J. A time-temperature relationship for rupture and creep stresses. Trans ASME. 1952;**74**:765-775

[25] Dorn J, Orr RL, Sherby O. Creep correlations of metals at elevated temperatures. AIME TRANS. 1954;**200**:71-80

[26] Shigley JE, Mischke CR. Mechanical Engineering Design. New York, USA: McGraw-Hill; 2003

[27] Chapra SC, Canale RP. Numerical Methods for Engineers. New York, USA: McGraw-Hill; 2006

[28] Manson S. A modified universal slopes equation for estimation of fatigue characteristics of metals. Journal of Engineering Materials and Technology. 1988;**110**:55

[29] Kanchanomai C, Miyashita Y, Mutoh Y. Low-cycle fatigue behavior of Sn-Ag, Sn-Ag-Cu, and Sn-Ag-Cu-Bi lead-free solders. Journal of Electronic Materials. 2002;**31**:456-465

[30] Shohji I, Yoshida T, Takahashi T, Hioki S. Tensile properties of Sn-Ag based lead-free solders and strain rate sensitivity. Materials Science and Engineering: A. 2004;**366**:50-55

[31] Patil R, Anand S. Thermo-structural fatigue analysis of shell and tube type heat exchanger. International Journal of Pressure Vessels and Piping. 2017;**155**:35-42

[32] Zhao X, Zhou Y, Yuan K. Creep-fatigue damage evaluation of Ni-based superalloy inconel 617 based on finite element analysis. 23rd International Conference on Nuclear Engineering: Nuclear Power - Reliable Global Energy, ICONE 2015, May 17–21, 2015. Chiba, Japan: American Society of Mechanical Engineers (ASME); 2015. p. et al.; GLSEQ, LLC/SCI Technologies. Inc; Hitachi-GE Nuclear Energy, Ltd.; Mitsubishi Heavy Industries, Ltd. (MHI); Toshiba Corporation; Westinghouse Electric Company

[33] Kumar RR, Pandey K. Static structural and modal analysis of gas turbine blade. International Conference on Advanced Material Technologies; 2016

[34] Madhu P. Stress analysis and life estimation of gas turbine Blisk for different materials of a jet engine. International Journal of Science and Research. 2016;**5**:1103-1107

[35] Tulsidas D, Shantharaja M, Kumar K. Design modification for fillet stresses in steam turbine blade. International Journal of Advances in Engineering & Technology. 2012;**3**: 343-346

[36] Che F. Material characterization and low cycle fatigue model of low Ag content lead-free solder. IEEE. Transactions on Device and Materials Reliability. 2017

[37] Hsieh MC. Modeling correlation for solder joint fatigue life estimation in wafer-level chip scale packages. Microsystems, Packaging, Assembly and Circuits Technology Conference (IMPACT), 2015 10th International: IEEE; 2015. pp. 65–8

[38] Khan SBaARA. Fatigue and creep interaction in steam turbine bladed disk. International Journal of Innovative Research in Science, Engineering and Technology. 2014;**3**

[39] Vava G. Simple Rotor Blisk. 2016; Available from: https://grabcad.com/library/simple-rotor-blisk-1

[40] Metals S. Inconel alloy 718. Publication Number SMC-045 Special Metals Corporation. 2007

[41] Dowling NE. Mechanical Behavior of Materials: Engineering Methods for Deformation, Fracture, and Fatigue. London, UK: Pearson; 2012

[42] Hattori H, Kitagawa M, Ohtomo A. Effect of grain size on high temperature low-cycle fatigue properties of inconel 617. Tetsu to Hagane. 1982;**68**:2521-2530